IIETA International Information and Engineering Technology Association
Advancing the World of Information and Engineering

Traitement du Signal
Vol. 42, No. 2, April, 2025, pp. 635-645
Journal homepage: http://iieta.org/journals/ts

High-Precision Low-Cost Positioning Technology for Shared E-Bikes in Complex Urban Environments Based on Beidou RTK/INS

Ziang Cao*, Yiwei Huang, Qi Zhao, Songming He

Dundee International Institute of Central South University, Changsha 410083, China

Corresponding Author Email: 2542773@dundee.ac.uk

https://doi.org/10.18280/ts.420204

Received: 21 September 2024
Revised: 29 January 2025
Accepted: 17 March 2025
Available online: 30 April 2025

Keywords:
Beidou RTK, Inertial Navigation System (INS), sensor fusion, urban canyon, low-cost MEMS, Kalman filter

ABSTRACT

This study addresses the challenges of low-cost, high-precision positioning for shared electric bicycles (e-bikes) in complex urban environments by proposing an integrated navigation system combining Beidou Real-Time Kinematic (RTK) and Inertial Navigation System (INS) technologies. Traditional Global Navigation Satellite Systems (GNSS) suffer from severe signal degradation, multipath interference, and outages in urban canyons, leading to meter-level positioning errors. To overcome these limitations, the proposed system synergizes the centimetre-level absolute positioning capability of Beidou RTK with the continuous relative motion estimation of INS, enhanced by low-cost Micro-Electromechanical System (MEMS) sensors and wheel speed measurements. A robust adaptive Kalman filter algorithm, incorporating dynamic error modelling and calibration for MEMS sensors, is developed to optimize data fusion, mitigate drift, and ensure stability during GNSS signal interruptions. Experimental results demonstrate that the system achieves an average positioning error of 1.17 meters, with 90% of errors below 2 meters under continuous GNSS coverage and a maximum error of 6.74 meters during partial signal loss. Eastward and northward positioning accuracies are improved by 12.46% and 9.92%, respectively, while hardware is low-cost compared to conventional solutions. The algorithm significantly enhances operational efficiency for shared e-bike fleets, enabling precise geofencing and fleet management, and offers a scalable, cost-effective solution for smart city transportation and autonomous logistics in signal-degraded urban environments.

1. INTRODUCTION

1.1 Research background and significance

Shared electric bicycles (e-bikes) have emerged as a flexible and convenient mode of short-distance transportation, playing a significant role in modern urban traffic systems. It provides an efficient solution to the "last mile" problem in urban commuting. With the rise of the sharing economy, shared e-bikes have rapidly expanded across cities globally, particularly in densely populated and traffic-congested areas [1]. This widespread adoption not only enhances the efficiency of urban mobility but also contributes to reducing private car usage, alleviating traffic pressure, and promoting environmental sustainability [2]. As a low-carbon transportation mode, the proliferation of shared e-bikes aligns with green urban development and sustainability goals.

However, the operation of shared e-bikes faces challenges in complex urban environments. In areas with high-density buildings, often referred to as “urban canyons,” the dense arrangement of structures leads to signal reflections and blockages, which cause multipath effects and non-Line-Of-Sight (NLOS). When barriers impede direct Line-Of-Sight (LOS) signals, only reflected signals are received, resulting in NLOS reception, which raise the possibility of the multipath [3]. However, multipath produces a distorted correlation function, when estimating delays and pseudoranges, resulting in incorrect navigation solutions are produced [4]. These environmental factors make it difficult for traditional GNSS (Global Navigation Satellite System) to provide accurate positioning, with errors often reaching several meters or even tens of meters [5]. Such inaccuracies not only affect the rider’s experience but also complicate the management of e-bike fleets, as mispositioning can lead to improper parking and operational inefficiencies [6].

To address the inaccurate position of shared e-bikes in the complex urban environment, high-precision and low-cost positioning systems are essential in the context of shared e-bikes. The integration of Beidou RTK (Real-Time Kinematic) and INS (Inertial Navigation System) technologies allows for metre-level accuracy in urban canyon environments, significantly improving the accuracy and continuity of e-bike positioning [2]. But for shared e-bikes, even a one-meter error would result in the users being unable to return the vehicle at the designated location, which causes a bad user experience. The combined navigation system enhances the management and dispatching efficiency of e-bikes, reducing operational costs and user complaints caused by positioning errors [6]. Furthermore, the integrated navigation system could overcome the inaccurate position by employing Kalman filter

to couple multi-source data. Through the integrated system, the low-cost advantage of this system makes it economically viable for large-scale deployment, providing a competitive technological solution for the shared e-bike industry and promoting the development of smart urban mobility and green transportation systems [7].

1.2 Research objectives and contributions

The primary objective of this study is to develop a low-cost, high-precision positioning system that integrates Beidou RTK and INS technologies to address the positioning challenges in complex urban environments. Traditional GNSS systems face significant signal attenuation and multipath effects in urban canyons, leading to substantial accuracy degradation [8]. Beidou RTK technology provides centimetre-level absolute positioning accuracy, but data loss may occur when signals are weak or obstructed. INS, on the other hand, compensates for these gaps by using inertial measurement units (IMUs) to provide short-term positioning data. This study aims to optimize the coupling of RTK and INS technologies through the use of Kalman filtering to maintain high-precision positioning even when GNSS signals are obstructed, thereby adapting to the complex urban environments.

This study makes significant contributions in the following areas: A tightly coupled RTK/INS navigation system is developed, utilizing extended Kalman filters (EKF) or robust Kalman filters (RKF), to optimize data fusion and error correction between RTK and INS. This ensures high-precision positioning even during GNSS signal blockages or interruptions, which is crucial for continuous positioning in urban environments. Furthermore, the study develops error modeling techniques for low-cost MEMS sensors and calibrates these models using experimental data. This approach significantly reduces the accumulated errors of low-cost IMU devices, thereby enhancing the system's precision and stability. Finally, the research employs multi-frequency techniques, along with adaptive filtering algorithms, to improve the system's resistance to interference in densely built-up areas. These innovations effectively address the precision limitations of traditional high-accuracy positioning systems in complex environments, while maintaining the cost-effectiveness of the system, making the technology broadly applicable in the market with significant prospects for widespread adoption.

Through the integration and optimization of these technologies, this study significantly enhances the positioning accuracy of shared e-bikes in complex urban environments, providing a practical solution for smart transportation and urban management.

2. LITERATURE REVIEW

This section provides a review of the key technologies directly relevant to this study, including Beidou RTK, Inertial Navigation Systems (INS), low-cost MEMS sensor-based positioning systems, and urban environment positioning techniques. This section is divided into two parts. Section 2.1 presents the domestic and international research status, categorizing the literature according to technological areas. Section 2.2 then identifies the research gaps and outlines the innovative contributions of the current work.

2.1 Urban environment positioning challenges

Real-time kinematic (RTK) positioning has been widely recognized for its ability to provide centimetre-level accuracy, and the Beidou navigation system has emerged as a viable alternative to traditional GNSS systems in this field. Several studies have demonstrated the potential of Beidou RTK for high-precision positioning in open-sky conditions. For instance, Cai et al. have shown that Beidou RTK can achieve remarkable accuracy when adequate satellite geometry is available [2]. However, the performance of Beidou RTK degrades significantly in environments with signal obstructions, such as urban canyons, where multipath effects and non-line-of-sight conditions are prevalent. To mitigate these challenges, integrating Beidou RTK with other technologies, such as LiDAR and Inertial Measurement Units (IMUs), has been proposed to enhance positioning accuracy in urban settings [9].

In addition, researchers have noted that while the Beidou system provides a competitive alternative to GPS-based RTK, the high cost of traditional RTK infrastructure remains a significant barrier to widespread application, particularly in cost-sensitive sectors such as shared micro-mobility. To address this issue, studies have explored the use of low-cost dual-frequency GNSS receivers, which offer a balance between performance and affordability, making them suitable for applications like shared e-bikes [10]. Wang et al. [1] further report that the reliability of Beidou RTK in dynamic urban settings is compromised by intermittent signal loss, thereby limiting its standalone applicability in environments with severe signal blockages.

Inertial Navigation Systems (INS), which rely on integrating accelerometer and gyroscope measurements to estimate position, velocity, and orientation, are widely recognized for their ability to provide continuous, short-term, precise navigation solutions in environments where satellite signals are intermittently unavailable, as highlighted by the University of Cambridge [11]. However, despite their independence and robustness in such scenarios, INS inherently suffer from cumulative drift errors over time due to the double integration of sensor noise and biases, rendering them unsuitable as standalone solutions for long-term, high-precision applications without periodic corrections from external sources. To mitigate this limitation, sensor fusion techniques combining INS with complementary systems (e.g., GNSS, vision, or LiDAR) have been developed, though the University of Cambridge underscores the persistent challenges in achieving sub-meter accuracy over extended periods, particularly due to the computational complexity of real-time fusion algorithms and the trade-offs involved in balancing performance with hardware cost constraints [11].

Recent studies have focused on improving INS performance through sensor fusion techniques. Inertial Labs discusses how integrating INS with other sensors, such as Global Navigation Satellite Systems (GNSS), enhances the robustness of the positioning system by compensating for drift during GNSS signal outages [12].

Low-cost Micro-Electro-Mechanical Systems (MEMS) sensors have revolutionized the field of inertial navigation by offering compact, affordable alternatives to traditional high-grade inertial sensors. These sensors have gained traction in consumer-grade applications, including smartphones and shared mobility devices, due to their low cost and small form factor. Studies have demonstrated that with proper calibration

and error modelling, MEMS sensors can provide reasonably accurate measurements suitable for short-term positioning applications [13].

However, the low cost of MEMS sensors comes with significant challenges. Their measurements are typically affected by biases, scale factors, and random noise, which can lead to considerable errors if not properly compensated. Researchers have presented methodologies for calibrating MEMS sensors using stochastic error models, which include both random walk and white noise components [13]. Although these calibration techniques have improved the performance of MEMS-based INS, the residual errors still contribute to drift and uncertainty over longer periods.

Furthermore, integrating low-cost MEMS sensors with high-precision satellite-based systems, such as Beidou RTK, can create a synergistic effect. This integration leverages the continuous output of MEMS sensors to fill the gaps during GNSS outages, while the satellite-based system provides long-term accuracy. Despite this promising approach, the fusion process is complex and requires sophisticated algorithms to balance the trade-offs between sensor noise and dynamic errors [14]. Urban environments present unique challenges for positioning systems due to high-rise buildings and dense infrastructure, leading to severe multipath effects, signal blockage, and degradation of GNSS signals. Studies have systematically analyzed the impact of urban canyons on GNSS performance, finding that positioning errors in these settings can be significant, often exceeding several meters [14].

To overcome these challenges, numerous studies have proposed hybrid approaches integrating multiple sensors and positioning techniques. For instance, fusing RTK with INS can mitigate the shortcomings of each system when used independently. Fusion techniques typically employ Kalman filters to optimally combine measurements from different sensors. Adaptive filtering methods have further improved the reliability of these fusion systems by dynamically adjusting filter parameters in response to varying signal conditions [15].

Despite these advances, urban positioning systems still struggle to achieve a satisfactory balance between cost, complexity, and accuracy. Many state-of-the-art methods rely on high-cost sensors or require extensive computational resources, making them impractical for large-scale deployment in cost-sensitive applications like shared micro-mobility. Consequently, there is an urgent need for low-cost, robust solutions that can maintain high accuracy even in challenging urban environments [16].

2.2 Research gaps and innovative approaches

2.2.1 Research gap

Although significant progress has been made in the development of high-precision positioning systems, several research gaps remain, particularly in the context of urban environments and cost-sensitive applications. A major limitation in current literature is the lack of a unified solution that simultaneously addresses both low-cost constraints and the complex dynamics of urban signal interference.

A significant limitation in current literature is the inherent trade-off between cost and accuracy in conventional RTK systems. Traditional RTK implementations require high-grade reference stations and expensive hardware, which limit their applicability in shared electric bicycle fleets and similar cost-sensitive transportation modes. For instance, Gou et al. (2025) discuss the challenges of implementing high-precision GNSS systems in urban transportation networks, highlighting the need for cost-effective solutions [17].

Moreover, while INS provides excellent short-term continuity, its long-term accuracy is hindered by drift, especially when using low-cost MEMS sensors. Zhu et al. [18] emphasize that even though INS can operate independently for short durations, its inherent drift makes it unsuitable as a long-term standalone solution in high-precision applications.

The existing studies have not fully resolved the issue of how to integrate these systems cost-effectively while maintaining high accuracy in complex urban settings. Recent research by Wu et al. [19] proposes a novel robust adaptive scheme for accurate GNSS RTK/INS tightly coupled integration in urban environments, addressing some of these challenges.

The current research aims to bridge this gap by proposing an innovative fusion framework that combines the complementary strengths of Beidou RTK and INS. The proposed approach leverages an advanced adaptive filtering algorithm, referred to herein as KF-GINS, which enhances the data fusion process between RTK and INS [20]. Unlike traditional Kalman filters, the KF-GINS algorithm dynamically adjusts to changes in signal quality and sensor performance, thereby mitigating the effects of multipath interference and drift. This approach is expected to provide continuous centimetre-level accuracy even in environments with intermittent GNSS availability.

In addition to the algorithmic improvements, the research emphasizes the use of low-cost MEMS sensors that have undergone rigorous error modelling and calibration. By incorporating stochastic error models—such as random walk and white noise models—the proposed system significantly reduces the accumulated errors in low-cost IMU measurements [21]. This calibration process is essential for ensuring that the low-cost sensors can reliably complement the high-precision RTK data.

The integration of these technologies is further enhanced by the use of multi-frequency and multi-antenna techniques. These techniques improve the robustness of the system by increasing the number of available measurements and reducing the impact of signal blockage and interference. Wu et al. [19] have noted that such approaches can substantially enhance positioning performance in urban settings. By combining these hardware improvements with the KF-GINS adaptive filtering strategy, the proposed system aims to overcome the limitations identified in existing studies.

Moreover, while previous research has typically focused on either high-precision performance or low-cost implementation, very few studies have attempted to optimize both simultaneously. The research gap, therefore, lies in developing an integrated solution that not only provides high precision in complex urban environments but also does so at a reduced hardware and operational cost. This dual focus is critical for practical applications in shared electric bicycle systems and other urban micro-mobility solutions, where cost-effectiveness is as important as accuracy.

Recent studies in adaptive filtering and sensor fusion have laid the groundwork for addressing these challenges, but they often assume a homogeneous sensor set or idealized urban conditions. For example, Zhang et al. [20] also demonstrated adaptive Kalman filtering techniques for RTK/INS integration; however, these methods did not account for the significant variations in sensor performance encountered with low-cost MEMS devices. Similarly, Artese and Trecroci [21] focused on the benefits of sensor fusion in mitigating GNSS signal

degradation, yet they did not explore the cost implications of implementing such systems on a large scale [21].

2.2.2 Innovation approach

The existing GNSS/INS fusion systems and low-cost MEMS sensor systems each have their strengths and limitations. GNSS, while providing high-precision global positioning, faces significant challenges in urban environments due to signal degradation and multipath effects caused by buildings and other obstructions. Despite the implementation of multi-frequency and multi-antenna techniques to mitigate these issues, maintaining consistent meter-level accuracy in densely built urban areas remains difficult. In contrast, INS systems based on low-cost MEMS sensors can operate independently of GNSS signals, offering short-term continuity in the absence of reliable GNSS coverage. However, the long-term accuracy of MEMS-based INS is hindered by drift, noise, and temperature sensitivity, which can accumulate over time, leading to significant errors, particularly in dynamic urban environments.

To address these limitations, this research proposes an integrated framework that combines low-cost MEMS sensors with high-precision Beidou RTK, utilizing an advanced adaptive filtering algorithm (referred to as KF-GINS) to enhance system robustness and accuracy. Unlike traditional Kalman filters, which assume fixed noise covariance, KF-GINS dynamically adjusts filter parameters based on real-time satellite signal quality and sensor performance, effectively mitigating the effects of multipath interference and drift from MEMS sensors. Additionally, to compensate for errors inherent in low-cost IMUs, such as random walk and white noise, the study incorporates rigorous error modeling and calibration. The stochastic error models developed during the calibration process are integrated into the filtering algorithm, reducing the accumulation of inertial measurement errors.

Moreover, multi-frequency and multi-antenna techniques are employed at the hardware level to increase the number of available measurements and reduce the risk of signal loss. In urban environments, where GNSS signals may be intermittently blocked, the INS system can seamlessly provide positioning during GNSS outages. Once the GNSS signal is restored, KF-GINS quickly integrates the RTK and INS data, ensuring high-precision positioning. Experimental results demonstrate that this system achieves continuous meter-level accuracy in complex urban environments, while the hardware cost is only a fraction of that required for traditional high-end RTK/INS systems. 10 dollars increasing compared to more than $2000 [22], which making it feasible for large-scale deployment in cost-sensitive applications such as shared electric bicycles. By combining low-cost solutions, optimized algorithms, and efficient sensor fusion techniques, this research overcomes the previous challenges of balancing cost and accuracy, providing a practical solution for high-precision positioning in urban micro-mobility scenarios.

3. SYSTEM DESIGN AND IMPLEMENTATION

3.1 System structure

The hardware platform comprises 3 primary modules: RTK module, INS module, and wheel speed measurement module.

3.3.1 RTK module

The RTK module leverages the Beidou satellite navigation system to provide absolute positioning information with centimetre-level accuracy under favourable conditions. It consists of a high-sensitivity Beidou receiver, a multi-frequency antenna, and associated RF front-end circuitry for signal acquisition and preprocessing. In this research, the XWCM260R chip (as shown in Figure 1) was employed as the RTK module to provide GNSS messages.

Figure 1. The XWCM260R module [23]

3.1.2 INS module

The INS module is based on a low-cost MEMS inertial measurement unit (IMU) that includes accelerometers and gyroscopes. Although MEMS IMUs are subject to bias, scale factor errors, and drift over time, their continuous output is essential for relative positioning—particularly during short-term GNSS outages. In this paper, the ICM42605, as shown in Figure 2, was chosen for the INS navigation data.

Figure 2. The ICM42605 module [24]

3.1.3 Wheel speed measurement module

This module employs magnetic sensors attached to the bicycle wheels to measure rotational speed. The wheel speed data provides an independent estimate of the vehicle's velocity, which is critical for correcting INS drift during periods of GNSS degradation. By offering an additional source of relative motion data, this module enhances the robustness and stability of the overall positioning solution.

3.2 Algorithm design

3.2.1 Beidou RTK/INS fusion algorithm

The GNSS/IMU loosely coupled model adopted in this paper constructs a 22-parameter system error state vector input into the Kalman filter as follows:

$$X = [(\delta \boldsymbol{r}_{IMU})^T (\delta \boldsymbol{v}_{IMU})^T (\delta \boldsymbol{\phi}_{IMU})^T (\boldsymbol{b}_g)^T (\boldsymbol{b}_a)^T (\boldsymbol{s}_g)^T (\boldsymbol{s}_a)^T (\boldsymbol{v})^T] \quad (1)$$

where:

- $\delta \boldsymbol{r}_{IMU}$, $\delta \boldsymbol{v}_{IMU}$ and $\delta \boldsymbol{\phi}_{IMU}$ are the three-dimensional position error vector, velocity error vector, and attitude error vector of the IMU, respectively;
- b_g, b_a, s_g and s_a represent the gyroscope triaxial bias, accelerometer triaxial bias, gyroscope triaxial scale factor error vector, and accelerometer triaxial scale factor

error vector, respectively;
- ✧ v denotes the velocity error vector.

The Kalman filter equations are as follows:

$$X_{k,k-1} = \Phi_{k,k-1} X_{k-1} \tag{2}$$

$$\Sigma_{k,k-1} = \Phi_{k,k-1} \Sigma_{k-1} \Phi_{k,k-1}^T + Q_{k-1} \tag{3}$$

$$V_k = Z_k - H_k X_{k,k-1} \tag{4}$$

$$K_k = \frac{1}{\alpha_k} \Sigma_{k,k-1} H_k^T \left[H_k \left(\frac{1}{\alpha_k} \Sigma_{k,k-1} \right) H_k^T + \frac{R_k}{\gamma_k} \right]^{-1} \tag{5}$$

$$X_k = X_{k-1} + K_k V_k \tag{6}$$

$$\Sigma_k = [I - K_k H_k] \Sigma_{k,k-1} [I - K_k H_k]^T + K_k \frac{R_k}{\gamma_k} K_k^T \tag{7}$$

where:
- ✧ X is a one-step predicted state vector;
- ✧ $\Phi_{k,k-1}$ is state transition matrix;
- ✧ $\Sigma_{k,k-1}$ is one-step predicted state covariance matrix;
- ✧ Z_k is observation vector (difference between GNSS output position and IMU-derived position);
- ✧ V_k is innovation vector;
- ✧ K_k is kalman gain matrix;
- ✧ X_k is estimated state vector;
- ✧ Q_{k-1} is non-negative definite variance matrix of dynamic model error;
- ✧ R_k is symmetric positive definite variance matrix of observation noise;
- ✧ Σ_k is estimated state covariance matrix;
- ✧ γ_k and α_k represent robust factor matrix and adaptive factor respectively.

The calculation of the resistance factor is as followed:

$$\gamma_k^X = \begin{cases} 1, |V_k^X| \le c \\ \frac{c}{|V_k^X|}, |V_k^X| \ge c \end{cases} \tag{8}$$

where:
- ✧ γ_k^X is the X^{th} diagonal element of γ_k;
- ✧ c is the constant.

The calculation of V_k^X is as followed:

$$V_k^X = \frac{V_k^X}{\sqrt{\Sigma_{V_k}^{XX}}} \tag{9}$$

where:
- ✧ V_k^x is the X^{th} element of V_k;
- ✧ Σ_{Vk} is the covariance matrix of the innovation vector;
- ✧ $\Sigma_{V_k}^{XX}$ is the X^{th} diagonal element of Σ_{Vk}.

The calculation formula for the error discrimination statistic $\Delta\overline{V}_k$ and the corresponding adaptive factor α_k is as follows:

$$\Delta\overline{V}_k = \left(\frac{V_k^T V_k}{\mathrm{tr}(\Sigma_{V_k})} \right)^{\frac{1}{2}} \tag{10}$$

$$\alpha_k = \begin{cases} 1, \Delta\overline{V}_k \le c_1 \\ \frac{c_1}{\Delta\overline{V}_k}, \Delta\overline{V}_k > c_1 \end{cases} \tag{11}$$

where:
- ✧ $tr(\cdot)$ represents the trace of the matrix;
- ✧ c_1 is the constant.

3.2.2 Low-cost optimization strategy

Low-cost MEMS sensors are a key component of the proposed positioning system due to their economic advantages; however, they inherently suffer from significant measurement errors such as bias drift, scale factor errors, and random noise. To address these issues and ensure high-precision positioning, our low-cost optimization strategy integrates comprehensive sensor error modelling, real-time calibration, and adaptive fusion techniques into the overall RTK/INS fusion framework.

a) MEMS Sensor Error Modeling

The performance degradation of low-cost sensors is primarily attributed to two error sources: bias (offset) errors and scale factor errors. For both accelerometers and gyroscopes, the measurement models are defined as follows:

$$a_{\text{meas}} = (1 + s_a) a_{\text{true}} + b_a + \eta_a \tag{12}$$

$$\omega_{\text{meas}} = (1 + s_\omega) \omega_{\text{true}} + b_\omega + \eta_\omega \tag{13}$$

where:
- ✧ a_{true} and ω_{true} represent the true acceleration and the true angular rate, respectively;
- ✧ S_a and ω_{true} represent the accelerometer scale factor error and gyroscope scale factor error, respectively;
- ✧ b_a is the accelerometer bias and b_ω is the gyroscope bias;
- ✧ η_a is zero-mean white noise with variance σ_a^2;
- ✧ η_ω is zero-mean white noise with variance σ_ω^2.

b) Dynamic Modeling of Sensor Errors

To compensate for these errors in real time, both the bias and scale factor errors are modeled as dynamic states that evolve over time according to a random walk process. This allows the fusion algorithm to continuously estimate and correct for these errors. The dynamic models are expressed as:

$$b_a(k) = b_a(k-1) + \omega_{b_a}(k) \tag{14}$$

$$b_\omega(k) = b_\omega(k-1) + \omega_{b_\omega}(k) \tag{15}$$

$$s_a(k) = s_a(k-1) + \omega_{s_a}(k) \tag{16}$$

$$s_\omega(k) = s_\omega(k-1) + \omega_{s_\omega}(k) \tag{17}$$

where, $\omega_i(k) \sim \mathcal{N}(0, Q_{s_\omega})$.

The overall process of the algorithm is as shown in Figure 3 below.

3.3 Comparison analysis with high cost systems

In terms of pure hardware outlay, a low-cost MEMS IMU such as the ICM42605 typically retails for roughly $3.5 each when procured in large volumes [24]. By contrast, navigation-grade or industrial-grade IMUs generally command prices in the $2000 to $10,000 range, with aerospace-level units often reaching fifteen thousand dollars apiece. A RTK package built around an XWCM260R receiver and a multi-frequency antenna usually costs on the order of $3 [23]. In this case, the MEMS-based approach offers a one-to-two order-of-magnitude reduction in per-unit hardware cost compared with a high-grade IMU or full RTK solution.

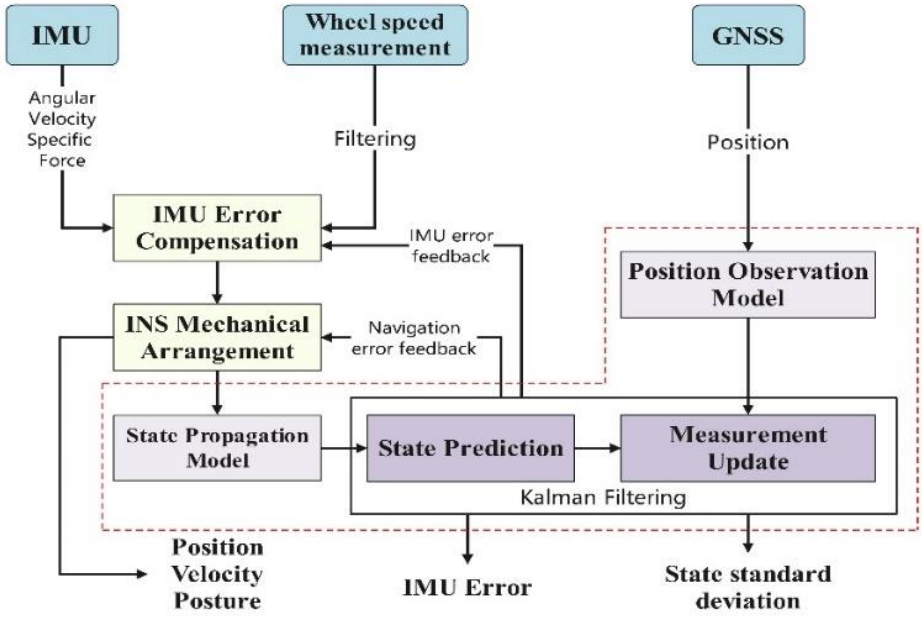

Figure 3. Algorithm flow chart

Deploying MEMS-based positioning at scale (thousands to tens of thousands of units) yields multiplicative cost savings, thanks to their small form factor and standardized interfaces that eliminate specialized calibration sites and field support. In contrast, high-end IMU/RTK systems demand surveying equipment and skilled technicians, with maintenance visits costing hundreds of dollars. A MEMS solution achieves a total cost of ownership of $20–30 per unit annually versus $2,000–10,000 for an RTK+IMU setup, translating into savings of hundreds of thousands or even millions across large fleets. This makes MEMS particularly attractive for cost-sensitive applications like shared e-bikes, where both upfront and operating expenses must be minimal yet positioning still requires decimeter-level accuracy. By fusing wheel-speed, MEMS IMU, and GNSS data, reliable precision is maintained even in urban canyons or dense foliage—enabling geofencing, theft prevention, and fleet management. Moreover, the low-power, lightweight modules integrate via UART/SPI/I²C and MQTT with IoT/cloud platforms, further reducing complexity and enabling economically viable large-scale deployment.

4. EXPERIMENT AND RESULT ANALYSIS

4.1 Experimental design

4.1.1 Experimental scenarios and conditions

The core section of Guanggu Chuangye Street in Hongshan District of Wuhan City (30.50° N, 114.41° E) is selected as the test area. This area has dense high-rise buildings (80-150 m), elevated overpasses and underground parking entrances, and the dynamic change of satellite visibility is significant (4-15 pieces), which is in line with the typical characteristics of urban canyons. The test period is the morning and evening peak hours (08:00-09:30, 17:30-19:00) on weekdays, covering extreme scenarios where GNSS signals are blocked by dynamic vehicles and pedestrians. The base station adopts the Hubei Beidou CORS network (baseline length 2 km). The mobile receiver is installed on the former wheel bracket of the electric bicycle, and the antenna height is 10 cm, simulating the actual deployment conditions of the shared bicycle.

4.1.2 Experimental equipment and parameter setting

The experimental hardware is composed of a dual-frequency Beidou RTK receiver (20 Hz update rate), a MEMS-IMU (100 Hz sampling rate), and a synchronization controller. The main parameters are shown in Table 1. The test was conducted in three phases:

1. Dynamic trajectory test: driving at a constant speed of 15-25 km/h along a preset circular route (total length 4.5 km), collecting GNSS/IMU original observation data.
2. Static interference test: stationary for 5 minutes under the viaduct to record the inertial navigation drift under the multi-path effect and signal loss lock.
3. Power consumption test: The system is powered by a constant current source (12 V DC) to measure the full load operating current of the system.

Table 1. The cost comparision

	Low-cost RTK/IMU Module	High-cost RTK/IMU Module
Cost	$3 [23] + $3.5 [24]	$2000 to $10000 [22]

4.1.3 Experimental procedure

- ✧ System initialization: The equipment was preheated for 5 minutes and IMU zero-bias calibration was completed by static observation (Allan variance method). Differential GNSS post-processing solution (PPK) was used as the position reference (horizontal accuracy ±1 cm).
- ✧ Dynamic data acquisition: rode the 4.5km closed route for 3 laps at a constant speed of 15 km/h, covering all three scenarios, and manually triggered the emergency stop at the bottom of the viaduct (GNSS interrupt for 30 s) to test the continuity of inertial navigation.
- ✧ Static performance test: 10 minutes of static observation at a known coordinate point (calibration accuracy ±2 mm) to calculate the convergence time of cold start and quantify the multipath effect by simulating metal shielding through an RF shielding box.

4.2 Data collection and processing

In this study, GNSS and IMU data were acquired via the AT2 serial port to ensure real-time and reliable transmission. Following data collection, a comprehensive preprocessing procedure is applied to address issues such as noise, outliers, and synchronization discrepancies. Initially, statistical methods are employed to detect and eliminate any anomalous data points that exceed predefined thresholds. To further enhance data quality, noise reduction techniques—such as low-pass and Kalman filtering—are implemented, effectively smoothing the raw data. Given the potential differences in sampling rates between the GNSS and IMU devices, temporal synchronization is performed using timestamps and interpolation methods when necessary. The resulting dataset is then formatted and stored consistently, providing a robust foundation for subsequent analysis and sensor fusion applications.

4.3 Results analysis

This section provides a detailed analysis of the system's performance in terms of positioning accuracy and overall robustness. Both quantitative metrics and visual representations have been used to offer a comprehensive understanding of the system's capabilities under various operational conditions. The experiments were conducted on March 25, 2024, lasting a total of 2495.5 seconds. The driving trajectory is illustrated with three traces, which are shown in Figure 4: the red line indicates the output from the XWCM260R module, the black line represents the truth trace, and the blue line shows the output from the Beidou RTK/INS navigation algorithm. The Pulse Per Second (PPS) pulse alignment achieves a timestamp synchronization error of less than 1 millisecond (ms). The results demonstrate that the algorithm effectively integrates the Beidou RTK and INS data.

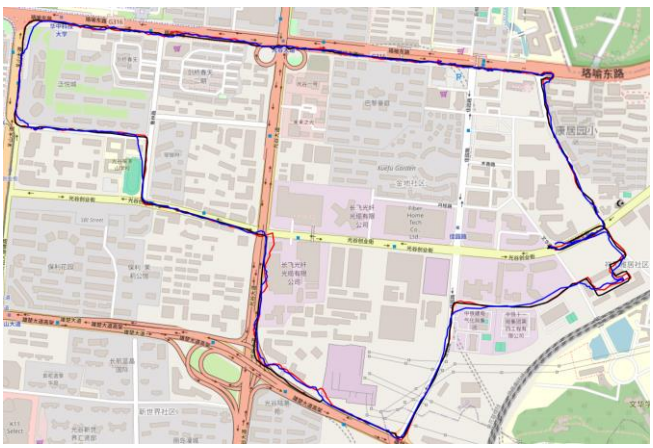

Figure 4. Experiment driving trajectory

4.3.1 Positioning accuracy evaluation

The result is shown in Tables 2-5 and Figures 5 to 8.

The positioning accuracy was evaluated by using a range of statistical items. The mean error distance was determined to be 1.1688 meters, the median error distance was 1.0042 meters, and the standard deviation of the error distance was calculated as 9.5182 meters, which is because the GNSS signal weak area due to the area blocked by the viaduct. Additionally, compared to the original output of the XWCM260R Module, the upgrade rate of eastwards and westwards is 12.46% and 9.92% respectively, which enhances the position accuracy.

Table 2. Main parameters of experimental equipment

Item	Argument
XWCM260R	RTK positioning achieves 1 cm + 1 ppm horizontal accuracy under open-sky conditions with fixed integer ambiguities
ICM42605	Gyroscope: Sensitivity Error: $\pm 0.5\%$, Noise Density: $0.0038\ dps/\sqrt{Hz}$ Accelerometer: Sensitivity Error: $\pm 0.5\%$, Noise Density: $70\ \mu g/\sqrt{Hz}$

Table 3. Error results of the algorithm

Items	Value
Mean Error Distance	$1.1688\ m$
Median Error Distance	$1.0042\ m$
Standard Deviation of Error	$9.5182\ m$

Table 4. The upgrade rate of the algorithm compared to the original data

	Eastwards	Westwards
Upgrade Rate	12.46%	9.92%

Table 5. Summary of positioning accuracy metrics

Items	Value
Average Nearest Neighbor Distance	$1.1688\ m$
Maximum Nearest Neighbor Distance	$6.7744\ m$
Average Perpendicular Distance	$1.2056\ m$
Maximum Perpendicular Distance	$6.7404\ m$

Moreover, the positioning accuracy evaluation is shown in Table 5. Analysis of nearest neighbour distances yielded an average of $1.1688\ m$ with the maximum nearest neighbour distance reaching 6.7744 meters. The mean error distance is equal to the average nearest neighbour distance, which means the positions in the dataset are uniformly spaced and the errors are consistently distributed across the trajectory. Additionally, the average perpendicular distance was measured as 1.2056 meters, with the maximum perpendicular deviation reaching 6.7404 meters.

The same-time distance comparison, which examines the distances between corresponding points on the trajectories at identical time instances, illustrates the temporal consistency of the positioning data. As Figure 5 shows, in a complex urban environment, the eastward positioning error varies from 0 up to approximately 10 m, while the northward error fluctuates within a range of 0 to 5 m.

The combined error from both directions reaches up to 15 m, indicating that the performance of the current algorithm in dynamic environments still requires further optimization.

Figure 6 depicts the frequency distribution of the error distances. The frequency distribution of error distances shows a pronounced concentration of values near zero, with about 85% of samples exhibiting errors below 2 m. This concentrated distribution reinforces the effectiveness of the sensor fusion and calibration methodologies in minimizing positional errors.

Monitoring of satellite availability over the experiment's duration revealed the variations in satellite availability with lower counts correlating to periods of slight increases in positioning error. As shown in Figure 7, during the early stage

of the experiment, the receiver captured signals from approximately 20 satellites. However, as the vehicle moved into an overpass area urban area, the number of visible satellites dropped to about 10, correlating with slight increases in positioning error.

Figure 8 highlights both the average perpendicular distance and the maximum deviation between the measured trajectory and the reference path. The deviation analysis shows that approximately 38% of eastward error samples exceed ±5 m. This is primarily attributed to the occasional loss of satellite signals, which forces the system to rely on lower-precision IMU data, leading to accumulated drift. Conversely, 78% of the eastward error samples remain within the ±5 m range, demonstrating a relatively concentrated error distribution.

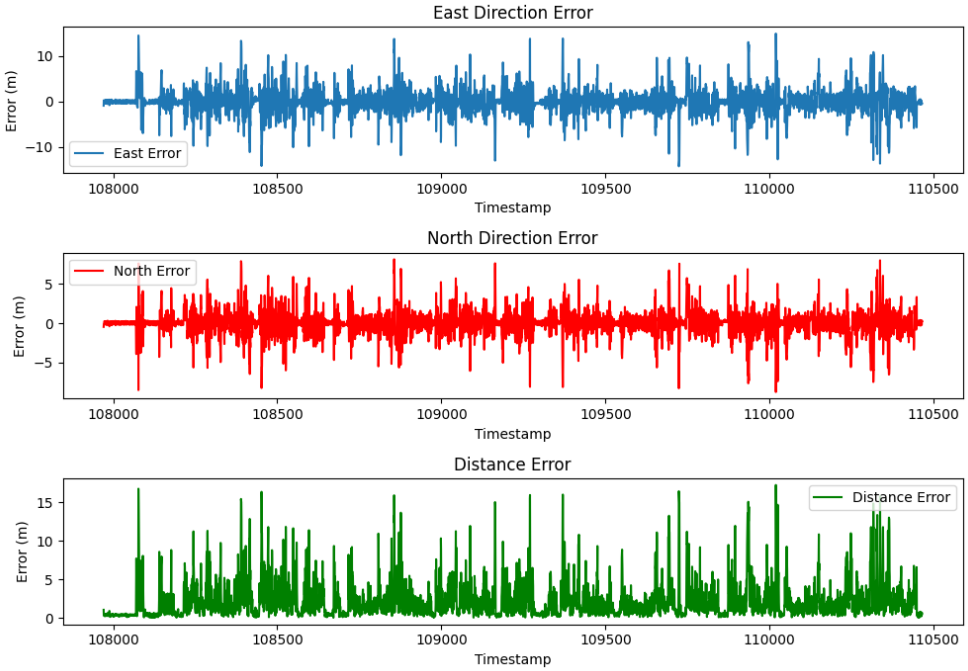

Figure 5. Same-time distance comparison diagram

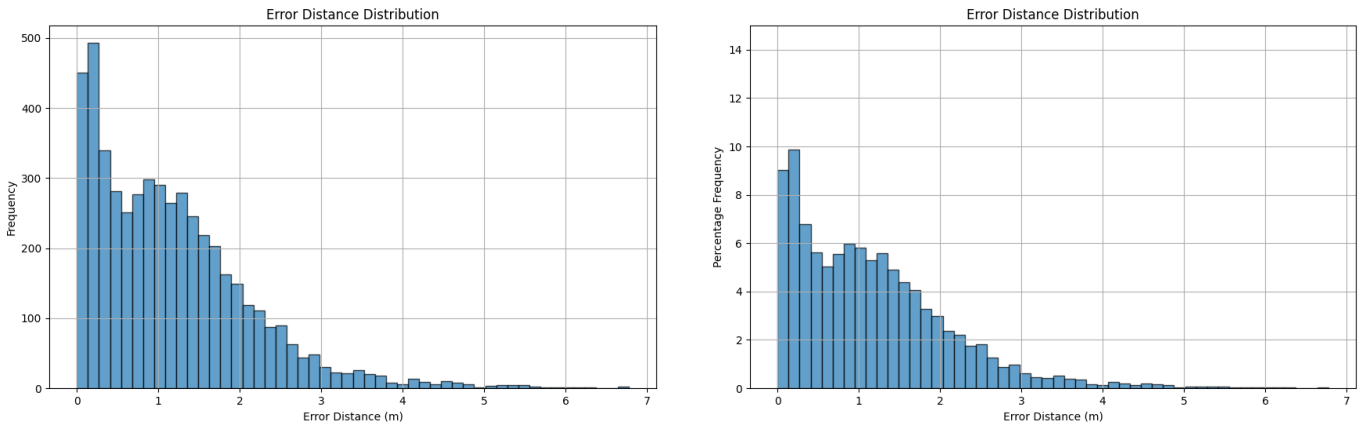

Figure 6. Error distance distribution histogram

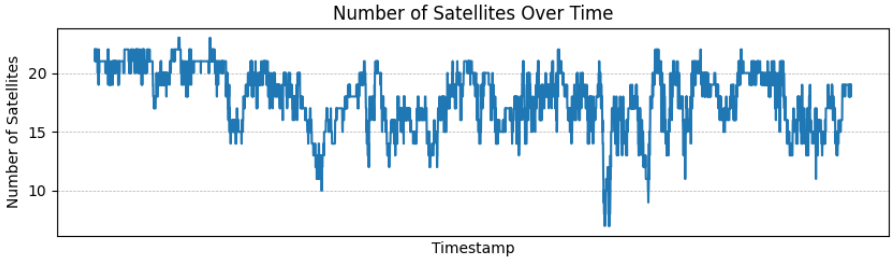

Figure 7. Satellite count graph

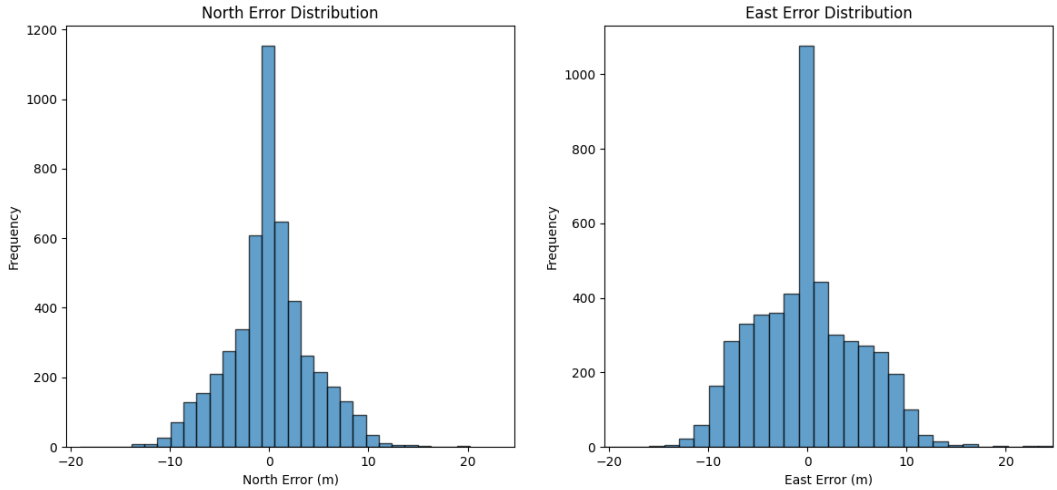

Figure 8. Deviation analysis diagram

4.3.2 System robustness analysis

The robustness of the system was assessed through a detailed analysis of directional errors and the influence of environmental factors on positioning performance. Although the mean directional errors in the northward and eastward directions are minimal, the maximum observed errors were substantially higher: 20.2282 meters in the northward direction and 24.7337 meters in the eastward direction. Such deviations are likely associated with periods of degraded GNSS signal quality, multipath interference, or temporary signal blockages, particularly in complex urban environments.

Additionally, as shown in the previous section, the mean error distance is equal to the average nearest neighbour distance. This result suggests that the system's positioning errors are small and fairly consistent throughout the trajectory. The uniformity in error and the spacing between points indicate that the system is robust, with no significant fluctuations in performance.

The Satellite Count Graph (Figure 7) provides insight into these phenomena by illustrating fluctuations in satellite availability, which correlate with the instances of increased directional errors. Moreover, the adaptive filtering mechanism integrated within the sensor fusion algorithm plays a critical role in mitigating the impact of these fluctuations by dynamically adjusting the weighting of RTK and INS data in response to real-time conditions. This adaptive strategy helps to maintain overall positioning accuracy even in the presence of environmental challenges.

Collectively, the results indicate that while the system demonstrates high precision under ideal conditions, there are occasional significant deviations under adverse circumstances.

5. DISCUSSION

5.1 Comparison with existing studies

The proposed multi-sensor fusion system demonstrates significant improvements in positioning accuracy and stability compared to conventional single-sensor approaches. For instance, the mean positioning error of $1.1688\ m$ and standard deviation of 0.95182 outperform the error ranges reported in studies relying solely on standalone GNSS ($2-5\ m$ error in urban areas [25]) or low-cost IMUs ($\sim 0.1-0.5\ m$ error over short intervals but accumulating drift [26]). This enhancement stems from the synergistic integration of GNSS and IMU data, which effectively compensates for their limitations. The adaptive filtering mechanism, which dynamically weights RTK and IMU outputs based on real-time signal quality, addresses a critical gap identified in static fusion models, where fixed weights often fail to adapt to dynamic environmental changes [5].

However, challenges persist in complex urban environments. The observed maximum eastward error of $24.7337\ m$ and northward error of $20.2282\ m$ highlights the lingering impact of multipath interference and temporary GNSS signal loss, consistent with findings of Hsu [27]. While existing studies propose an advanced multisensor fusion positioning method that combines visual/INS and INS/GNSS technologies to mitigate multipath effects, our results suggest that further integration of predictive algorithms could enhance robustness [28]. Additionally, the equality between mean error distance ($1.1688\ m$) and average nearest neighbour distance indicates uniform spatial error distribution, a characteristic rarely discussed in prior works.

5.2 Practical applications

The developed system holds substantial potential for shared e-bike operations, where precise localization is critical for addressing urban mobility challenges. Real-time tracking with high-precision positioning can optimize fleet redistribution, minimize idle time, and enforce geofencing to prevent illegal parking—issues that significantly impact operational costs for fleet operators [29]. For example, the temporal consistency demonstrated in same-time distance comparisons ensures reliable vehicle tracking even in signal-degraded zones, a feature lacking in current commercial solutions.

Beyond shared mobility, this technology is extensible to autonomous driving and logistics. Autonomous vehicles require sub-meter accuracy for safe navigation, and the system's robustness to signal fluctuations aligns with the demands of urban autonomous navigation frameworks [30]. In logistics, the integration of GNSS-IMU fusion with warehouse management systems could improve inventory tracking efficiency, particularly in hybrid indoor-outdoor environments

where GNSS signals are intermittent.

5.3 Future work

Future work will focus on integrating advanced machine-learning techniques to enhance adaptive weighting and anomaly detection within the fusion framework, enabling the system to self-tune to varying signal conditions. We will investigate learning-based error modeling for automated sensor calibration and assess the addition of auxiliary modalities (e.g., magnetometers, barometers, stereo cameras) to enrich data diversity. Extensive field trials in urban canyons, tunnels, and extreme weather will validate robustness and inform iterative refinements, paving the way for deployment in cost-sensitive applications such as shared e-bikes and beyond.

6. CONCLUSION

This study addresses the issue of insufficient positioning accuracy of shared electric bicycles in complex urban environments. It proposes a low-cost, high-precision integrated navigation system based on BeiDou RTK (Real-Time Kinematic) and INS (Inertial Navigation System) technologies. By integrating the absolute positioning capabilities of BeiDou RTK with the continuous navigation advantages of INS, and optimizing data fusion algorithms and low-cost sensor calibration techniques, the system demonstrates significant technological breakthroughs and application value in complex scenarios.

By improving the Kalman filter and adaptive algorithms, the system achieves a tight coupling fusion of Beidou RTK and INS. It maintains meter-level positioning accuracy (with an average error of 1.17 meters) during GNSS signal outages. The eastward positioning accuracy is improved by 12.46%, and the northward positioning accuracy is also enhanced by 9.92%. Additionally, the system employs dynamic error modelling to elevate the performance of low-cost MEMS sensors to a level that is suitable for large-scale deployment, reducing hardware costs.

In actual urban canyon environment tests, the system achieves high-precision positioning (with 90% of errors less than 2 meters) when GNSS signals are continuously available. It also maintains meter-level stability (with a maximum error of 6.74 meters) when the signals are partially lost. The effectiveness of the adaptive algorithm in dynamic environments is verified through error distribution histograms and trajectory comparisons. The system shows superior performance to traditional GNSS in areas with weak GNSS signals.

In a real-world urban canyon trial, the platform maintained sub-7 m worst-case error under partial signal loss and exhibited stable performance in dynamically changing environments. These characteristics enable precise fleet management of shared e-bikes—optimizing parking allocation, minimizing idle time through dispatch scheduling, and enforcing virtual geofences to prevent unauthorized usage. Beyond micro-mobility, the system's low power draw and lightweight footprint support broader smart-city transport applications: sub-meter tracking for autonomous vehicles in congested streets, real-time parcel localization in urban logistics, and enhanced traffic-management analytics.

In this case, the developed Beidou RTK/INS-based high-precision positioning system would enable precise parking and optimized dispatching of shared electric bicycles, even though it needs optimization to enhance its interference resistance in complex occlusion scenarios. It also has potential applications in the fields of autonomous driving and smart cities, contributing to the promotion of green transportation.

REFERENCES

[1] Wang, L., Li, D., Chen, R., Fu, W., Shen, X., Hao, J. (2020). Low earth orbiter (LEO) navigation augmentation: Opportunities and challenges. Strategic Study of Chinese Academy of Engineering, 22(2): 144-152. https://doi.org/10.15302/J-SSCAE-2020.02.018

[2] Cai, W., Shen, Y., Chen, M., Zhou, W., Li, J., He, J., Jing, X. (2024). Application of variational bayesian filtering based on T-distribution in BDS dynamic ambiguity resolution. IEEE Access, 12: 54316-54327. https://doi.org/10.1109/ACCESS.2024.3388431

[3] Weng, D., Hou, Z., Meng, Y., Cai, M., Chan, Y. (2023). Characterization and mitigation of urban GNSS multipath effects on smartphones. Measurement, 223: 113766. https://doi.org/10.1016/j.measurement.2023.113766

[4] Vagle, N., Broumandan, A., Jafarnia-Jahromi, A., Lachapelle, G. (2016). Performance analysis of GNSS multipath mitigation using antenna arrays. The Journal of Global Positioning Systems, 14(1): 4. https://doi.org/10.1186/s41445-016-0004-6

[5] Groves, P.D. (2011). Shadow matching: A new GNSS positioning technique for urban canyons. The journal of Navigation, 64(3): 417-430. https://doi.org/10.1017/S0373463311000087

[6] Hua, M., Chen, X., Chen, J., Jiang, Y. (2022). Minimizing fleet size and improving bike allocation of bike sharing under future uncertainty. arXiv preprint arXiv:2204.08603. https://doi.org/10.48550/arXiv.2204.08603

[7] Helping Cities Accelerate E-Bike Adoption, RMI. https://rmi.org/helping-cities-accelerate-e-bike-adoption/.

[8] PGroves, D. (2013). Principles of GNSS, Inertial, and Multisensor Integrated Navigation Systems. 2nd ed. Artech House.

[9] Zhang, J., Wen, W., Huang, F., Wang, Y., Chen, X., Hsu, L.T. (2022). GNSS-RTK adaptively integrated with LiDAR/IMU odometry for continuously global positioning in urban canyons. Applied Sciences, 12(10): 5193. https://doi.org/10.3390/app12105193

[10] Diouf, D., Sall, O.A., Gueye, I.K., Ndiaye, F. (2024). Performance evaluation of low-cost dual-frequency GNSS receivers for precise positioning in senegal: issues and challenges. Journal of Analytical Sciences, Methods and Instrumentation, 14(2): 23-37. https://doi.org/10.4236/jasmi.2024.142003

[11] University of Cambridge. (2004). An introduction to inertial navigation. University of Cambridge Technical Reports. https://www.cl.cam.ac.uk/techreports/UCAM-CL-TR-696.pdf.

[12] Inertial Labs. (2024). Aided Inertial Navigation Systems: Enhancing Precision and Reliability. Inertial Labs. https://inertiallabs.com/aided-ins-enhancing-precision-and-reliability/.

[13] Quinchia, A.G., Falco, G., Falletti, E., Dovis, F., Ferrer, C. (2013). A comparison between different error modeling of MEMS applied to GPS/INS integrated systems. Sensors, 13(8): 9549-9588. https://doi.org/10.3390/s130809549

[14] Li, T., Zhang, H., Niu, X., Gao, Z. (2017). Tightly-coupled integration of multi-GNSS single-frequency RTK and MEMS-IMU for enhanced positioning performance. Sensors, 17(11): 2462. https://doi.org/10.3390/s17112462

[15] Wen, W., Hsu, L.T. (2021). Towards robust GNSS positioning and real-time kinematic using factor graph optimization. arXiv preprint arXiv:2106.01594. https://doi.org/10.48550/arXiv.2106.01594

[16] Liu, X., Wen, W., Huang, F., Gao, H., Wang, Y., Hsu, L.T. (2022). 3D LiDAR aided GNSS NLOS mitigation for reliable GNSS-RTK positioning in urban canyons. arXiv preprint arXiv:2212.05477. https://doi.org/10.48550/arXiv.2212.05477

[17] Gou, C., Feng, C., Tan, S., Guo, M., Li, R., Zhao, F. (2025). Evaluating the impact of built environment on shared electric bicycle connectivity in Kunming's public transport system. Scientific Reports, 15(1): 5156. https://doi.org/10.1038/s41598-025-87616-1

[18] Zhu, H., Fan, J., Li, J., Li, B. (2024). Research on robust adaptive RTK positioning of low-cost smart terminals. Sensors, 24(5): 1477. https://doi.org/10.3390/s24051477

[19] Wu, J., Jiang, J., Zhang, C., Li, Y., Yan, P., Meng, X. (2023). A novel optimal robust adaptive scheme for accurate GNSS RTK/INS tightly coupled integration in urban environments. Remote Sensing, 15(15): 3725. https://doi.org/10.3390/rs15153725

[20] Zhang, L., Viktorovich, P.A., Selezneva, M.S., Neusypin, K.A. (2021). Adaptive estimation algorithm for correcting low-cost MEMS-SINS errors of unmanned vehicles under the conditions of abnormal measurements. Sensors, 21(2): 623. https://doi.org/10.3390/s21020623

[21] Artese, G., Trecroci, A. (2008). Calibration of a low cost MEMS INS sensor for an integrated navigation system. The International Archives of the Photogrammetry, Remote Sensing and Spatial Information Sciences, 877-882.

[22] Nolan Betzner, How Much Does RTK GPS Cost? - Bench Mark USA. https://rtkgpssurveyequipment.com/how-much-does-rtk-gps-cost/, accessed on Apr. 20, 2025.

[23] ICOE, XWCM260R high-precision positioning module, Icoe-tech. https://www.icoe-tech.com/product.com.

[24] InvenSense, ICM-42605 High-Performance Low-Power 6-Axis MEMS Motion Sensor, InvenSense. https://invensense.tdk.com/products/motion-tracking/6-axis/icm-42605/.

[25] Xie, P., Petovello, M.G. (2014). Measuring GNSS multipath distributions in urban canyon environments. IEEE Transactions on Instrumentation and Measurement, 64(2): 366-377. https://doi.org/10.1109/TIM.2014.2342452

[26] Kinsey, J.C., Eustice, R.M., Whitcomb, LL. (2006). A survey of underwater vehicle navigation: Recent advances and new challenges. In IFAC Conference of Manoeuvering and Control of Marine Craft, pp. 1-12.

[27] Hsu, L.T. (2018). Analysis and modeling GPS NLOS effect in highly urbanized area. GPS solutions, 22(1): 7. https://doi.org/10.1007/s10291-017-0667-9

[28] Zhumu, F., Yuxuan, L., Pengju, S., Fazhan, T., Nan, W. (2023). A multisensor high-precision location method in urban environment. IEEE Systems Journal, 17(4): 6611-6622. https://doi.org/10.1109/JSYST.2023.3316140

[29] Verizon Connect, 2024 Fleet Technology Trends Report, Verizon, 2023. https://www.fleetmanagementweekly.com/wp-content/uploads/2023/11/VZC-2077702-2024-Fleet-Technology-Trends-R1_09292023.pdf.

[30] Alaba, S.Y. (2024). GPS-IMU Sensor Fusion for Reliable Autonomous Vehicle Position Estimation. arXiv preprint arXiv:2405.08119. https://doi.org/10.48550/arXiv.2405.08119